Permafrost, Phillips, Springman & Arenson (eds)
© 2003 Swets & Zeitlinger, Lisse, ISBN 90 5809 582 7

Mountain permafrost and recent Alpine rock-fall events: a GIS-based approach to determine critical factors

J. Noetzli, M. Hoelzle & W. Haeberli
Glaciology and Geomorphodynamics Group, Department of Geography, University of Zurich, Switzerland

ABSTRACT: Glacier retreat and permafrost changes, as related to climate change, are supposed to affect stability conditions of steep rock walls in cold mountain ranges. Several rock-fall events, which have occurred in the European Alps during the 20th century, are possibly related to warm permafrost. This study undertakes a systematic parameterization of rock-fall events in order to increase information about thermal and topographic conditions under which rock instabilities develop in areas of mountain permafrost. Thermal conditions of historically documented starting zones are parameterized by applying either empirical rules or GIS-based spatial models; slope is derived from DTMs. Despite the relatively small number of events documented so far (around 20), the first results presented clearly indicate that the factor permafrost must be considered in connection with rock-falls from high mountain slopes.

1 INTRODUCTION

A number of periglacial rock-fall events have occurred in the European Alps during the 20th century such as the Brenva Glacier rock avalanches of 1920 and 1997 in the Aosta Valley or the recent instability in the Monte Rosa east wall in the Anzasca Valley, both in the Italian Alps. These events are possibly related to warm permafrost. Glacier retreat and changes in permafrost, as related to present atmospheric warming, may destabilize oversteepened rock walls and accelerate cliff retreat in high mountain areas (Haeberli et al. 1997).

The influence of permafrost on the destabilization of rock walls is a very young field of research. The most important processes concern (a) fracturing of rock during seasonal and multiannual freezing, (b) changes in hydraulic conductivity, pore-water pressure and circulation during freezing and thawing, and (c) changes in surface geometry from major rock-falls (Haeberli et al. 1997). Davies et al. (2001) showed in a series of direct shear box tests that a rise in ground temperature might lead to a reduction in the shear strength of ice-bonded discontinuities and an associated reduction in the factor of safety of the slope, which could result in slope failure even whilst there is still ice in the joints. Slope stability might, therefore, be very sensitive to changes in the thermal environment, especially where unfrozen water is present in partially ice-filled bedrock fissures is present (Davies et al. 2001).

However, available knowledge about thermal, topographic and geological conditions under which such instabilities develop remains limited and needs quantitative information. In order to proceed in this direction, parameters are determined in a systematic study of known rock-fall events in the Alps. In a first step, historically documented starting zones are investigated.

2 HISTORICAL ROCK-FALL EVENTS

So far, twenty rock-fall events or slope instabilities have been documented (Table 1, Fig. 1). Nine events are located in the Swiss Alps, ten in the Italian Alps and one occurred in the German Wettersteingebirge. Except Triolet (1717), they all took place in the 20th and the beginning of the 21st century.

The affected rock walls are located higher than 2000 m a.s.l. and are above the tree line (Fig. 2). Most of them are situated within the permafrost altitudinal belt. In the more recent scientific literature permafrost-related processes such as ground-ice melt due to climatic warming and connected changes in groundwater regimes have repeatedly been suggested to activate such rock falls (Deline 2001, Dramis et al. 1995, Geotest 2000, Wegmann 1998). In some deposits, even ice blocks were present (for example, Val Pola and Mättenberg; Dramis et al. 1995, Geotest 2000).

Historically documented starting zones and run out paths of the events are collected and stored in vector format within the ARC/INFO GIS software. Converted to grid format, this data then serves as a basis for the following cell-based spatial modelling of critical factors. For most analyses, digital terrain models (DTMs) are needed. For the analysis of the events in the Swiss Alps the DHM25 Level2 from the Swiss Federal Office of Topography was used. For the Italian events, DTMs were created based on the maps of the Swiss Federal Office of Topography 1:50,000. All DTMs and cell-based calculations have a resolution of 25 m.

Table 1. Geomorphometric parameters of the rock-fall events considered. The altitude relates to the uppermost point of the starting zone. H is the fall from the top of the scarp to the bottom of the accumulation, L the corresponding horizontal travel distance. The star in column Gl. indicates events that are situated in glacial environment.

n.	Name	Date	Altitude (m a.s.l.)	Aspect	Volume (10^6. m^3)	H (m)	L (m)	H/L	Gl.	Reference
1	Triolet (I)	1717	3600	E	16–20	1860	7200	0.26	*	Porter & Orombelli 1980
2	Fletschhorn (CH)	1901	3615	NE	0.8	2115	5500	0.38	*	Coaz 1910
3	Brenva I (I)	1920	4200	E	2–3	2750	5000	0.55	*	Deline 2001
4	Felik (I)	1936	3585	SW	0.2	1250	3000	0.42	*	Dutto & Mortara 1991
5	Jungfrau (CH)	1937	3800	SE	0.15	435	1200	0.36	*	Alean 1984, Wegmann 1998
6	Matterhorn (I)	1943	4150	SE	0.24	1000	850	1.18		Vanni 1943
7	Miage I (I)	1945	3050	NE	0.3	730	1700	0.43	*	Deline 2002
8	Becca di Luseney (I)	1952	3150	SW	1	1650	3800	0.43	*	Dutto & Mortara 1991
9	Druesberg (CH)	1987	2100	NW	0.07	300	700	0.43		Wegmann 1995
10	Val Pola (I)	1987	2360	NE	33–35	1250	3470	0.36		Dramis et al. 1995
11	Tschierva (CH)	1988	3280	SW	0.3	550	1000	0.55	*	Schweizer 1990
12	Piz Serscen (CH)	1988	3750	SE	?	500	1250	0.40	*	M. Spillmann, Geotest (pers. comm.)
13	Randa (CH)	1991	2300	SE	30	1020	1400	0.73		Schindler et al. 1993
14	Miage II (I)	1991	3000	NW	0.3	550	1100	0.50	*	Deline 2002
15	Zuetribistock (CH)	1996	2250	E	1.1	900	1250	0.72		Keller 1996, Kobel 1996
16	Brenva II (I)	1997	3725	SE	2	2285	5760	0.40	*	Deline 2001
17	Mättenberg (CH)	2000	2720	NW	0.1	800	1200	0.67		Geotest 2000
18	Zugspitze (D)	2001	2630	N	0.03	600	?	?		O. Mustafa, Univ. Jena (pers. comm)
19	Monte Rosa (I)	2001	3100	E	0.005	700	1250	0.56	*	this paper
20	Gruben (CH)	2002	3520	NW	0.1	530	1125	0.47	*	this paper

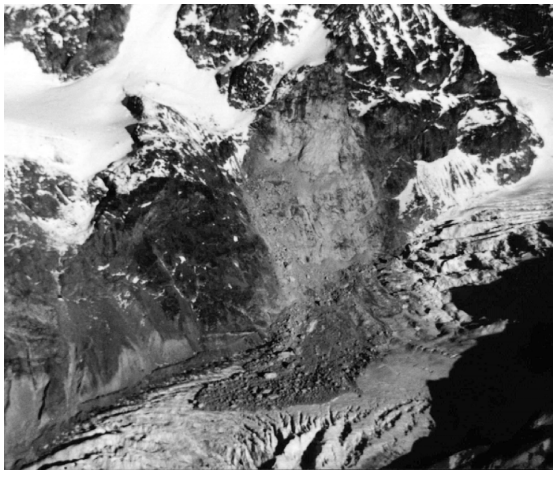

Figure 1. Rock fall from permafrost slopes at Piz Morteratsch (Eastern Swiss Alps, Event 11) onto Tschierva Glacier. Foto by J. Schweizer, autumn 1988.

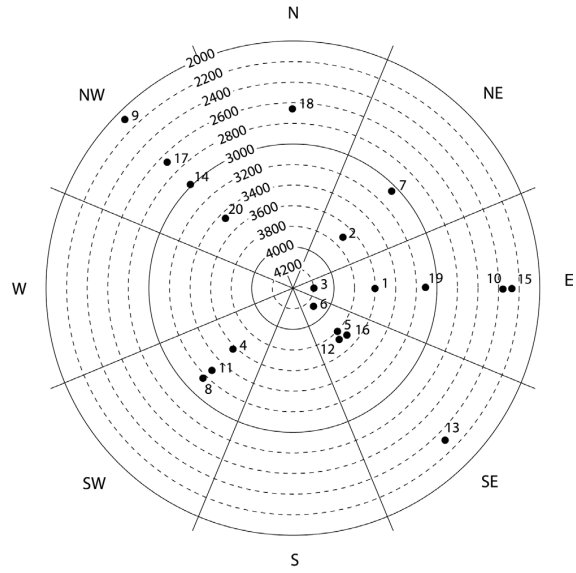

Figure 2. Altitude of starting zones related to slope exposition. The numbers of the events refer to those in Table 1.

3 CALCULATIONS

3.1 *Thermal conditions*

The two approaches applied to estimate thermal conditions at the scarp are both based on mean annual air temperature (MAAT) and potential direct solar radiation, the two most dominating factors governing permafrost occurrence. Surface temperatures of rock walls are a result of the energy balance at the rock surface. The decisive factors determining the surface temperature of a rock wall are aspect (shortwave radiation), altitude (sensible heat and longwave incoming radiation) and lithology (type of surface; Wegmann 1998, Mittaz et al. 2000, Mittaz et al. 2002).

3.1.1 *Temperature calculation using empirical rules*

In a first approach to estimating the thermal conditions at the surface of the starting zones, the PERMAKART model (Keller 1992) is applied. PERMAKART is based on the so-called “rules of thumb” to predict local permafrost occurrence as developed earlier for

the Swiss Alps by Haeberli (1975). These rules of thumb primarily consider radiation effects as related to aspect, and air temperature as related to altitude.

As these empirical rules are deduced and calibrated for the Upper Engadine in the Eastern Swiss Alps, they are first fitted to different climate regions using 0°C-isotherm altitudes and temperature gradients for each region. Secondly, the altitude of the lower limit of permafrost existence is determined for each event by applying the adjusted rules. Then the altitude difference between the mean altitude of the starting zone to the respective permafrost limit is calculated. Based on the key assumption that the mean annual surface temperature (MAST) at the limit of permafrost existence is about 0°C, this height difference is converted to a temperature value using the same temperature gradients. The resulting temperature value (T1), the deviation of MAST to marginal permafrost conditions, is a first approximation to the temperature at the surface of the starting zone. As the accuracy of the rules of thumb lies in the range of 100 m, the one of this calculation is around 0.5°C. The main uncertainty related to this approach, however, is caused by the omission of complex topological effects (mountain shadow).

3.1.2 *Temperature calculation using the program PERMAMAP*

The second approach allows another estimation of the temperature conditions at the surface of the scarp, applying the GIS-based spatial model PERMAMAP. The calculations were done according to Frauenfelder & Kääb (2000) and Frauenfelder et al. (2001), who developed this method for calculating temperatures of rock-glacier fronts. The PERMAMAP model calculates permafrost limits based on a statistical relation between BTS-measurements, MAAT and potential direct solar radiation at the limit of permafrost existence (Hoelzle & Haeberli 1995, Hoelzle 1996). Based on this statistical relation, the altitude of the lower limit of permafrost occurrence is calculated for the local amount of radiation available at each scarp. The accuracy of the altitude of the lower permafrost limit depends on the resolution of the DTM that underlies the calculation. Based on a DTM with a resolution of 25 m, the accuracy lies in the range of a few meters. The temperature difference between the MAAT at the permafrost limit and the MAAT at the scarp is the deviation to Hoelzle & Haeberli's (1995) relation describing the limit of permafrost existence. Based on the same key assumption as the first method, this parameterized temperature value (T2) is a second approximation to the thermal conditions at the rock surface. Temperatures for Zugspitze have not been calculated because no adequate DTM is available yet. For the exact calculations cf. Noetzli (2003). The mean potential solar radiation for each starting zone is calculated using Funk & Hoelzle's (1992) model.

The accuracy of the model might be influenced by the fact that the statistical relation used is based on the mean potential direct solar radiation of the summer months and BTS-measurements. As the considered rock walls are too steep to keep any thicker snow cover, the statistical relation might not be exact for permafrost conditions and processes in steep rock walls.

3.2 *Slope*

The slope of each documented starting zone is derived from DTMs using the ARC/INFO-command SLOPE. Then statistical parameters including all cells of the starting zones are determined. Where no adequate digital terrain information is available, the slope can be estimated from maps (Zugspitze).

4 RESULTS

4.1 *Thermal conditions*

4.1.1 *Temperature calculation using the rules of thumb*

As Table 2 shows, calculated temperatures range from −6.3° to 5.9°C. The coldest scarp is the one in the northeast face of Fletschhorn, the starting zone of a combined ice/rock avalanche. Randa, Val Pola and Zuetribistock show warm temperatures several degrees above the freezing point. The other events show neither very warm nor very cold temperatures: 80% of the events have a parameterized temperature between −4° and +4° and 50% between −2° and +2°C, respectively.

4.1.2 *Temperature calculation using PERMAMAP*

For each scarp, the minimum, maximum and mean of the direct solar radiation vs. MAAT has been plotted in a xy-diagram (Fig. 3). Additionally, Hoelzle and Haeberli's (1995) relation of potential direct solar radiation to MAAT at the permafrost limit is displayed (full line in Fig. 3). The mean variation is rather high. The upper left point triple corresponds to the Fletschhorn-event and the lowest two to Randa (right) and Val Pola. These are the only two events completely outside permafrost area. The Zuetribistock-scarps are located at the permafrost limit. All other events are situated within – or close to – permafrost areas. As would be expected, some starting zones are located in warm permafrost areas, but events from cold permafrost areas also occurred.

The dotted line indicates a shift of Hoelzle's relation by about −2°C. This corresponds more or less to Davies' (2001) assumption that the factor of safety within ice-containing rock walls falls below unity if temperature rises above −1.4°C. Despite the great

Table 2. Surface temperatures estimated by applying the rules of thumb. PFH is the local altitude of the lower limit of permafrost occurrence for the given aspect. T_P is the MAAT at the mean altitude of the scarp, T1 is the parameterized surface temperature. ± indicates the range of T1 to the upper/lower boundary of the scarp.

n.	Name	PFH	T_P (°C)	T1 (°C)	± (°C)
1	Triolet	3252	−6.9	−0.89	1.2
2	Fletschhorn	2637	−9.2	−6.26	0.6
3	Brenva I	3253	−10.5	−3.74	2.0
4	Felik	2937	−8.1	−3.29	0.6
5	Jungfrau	2997	−9.6	−4.52	0.3
6	Matterhorn	3037	−11.8	−5.18	1.5
7	Miage I	2852	−3.6	0.01	1.2
8	Becca di Luseney	3152	−3.9	0.76	0.8
9	Druesberg	2102	−1.1	0.19	0.2
10	Val Pola	2600	−0.9	2.52	1.2
11	Tschierva	2900	−6.0	−1.90	0.2
12	Piz Scerscen	3000	−8.7	−3.64	0.6
13	Randa	3037	−0.4	5.92	1.5
14	Miage II	2652	−3.3	−1.79	0.3
15a	Zuetribistock I	2662	−2.1	3.16	0.8
15b	Zuetribistock II	2662	−1.8	3.25	0.6
16	Brenva II	3252	−7.6	−1.94	0.9
17	Mättenberg	2597	−3.1	−0.14	0.6
18	Zugspitze	2472	−3.2	−0.65	0.3
19	Monte Rosa	3037	−5.2	−0.08	0.3
20	Gruben	2437	−7.7	−6.26	0.2

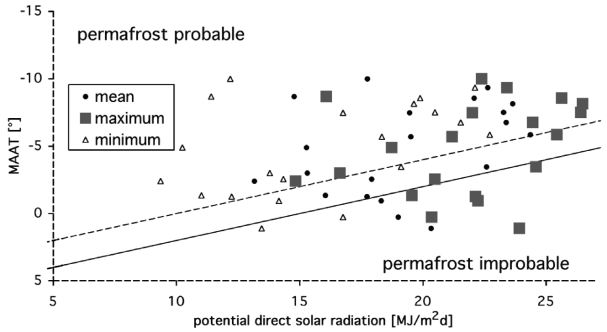

Figure 3. Diagram displaying the minimum, maximum and mean of the direct solar radiation vs. MAAT for each event and Hoelzle & Haeberli's (1995) relation of potential direct solar radiation to MAAT at the permafrost limit (full line). The dotted line corresponds to a shift of this line by about −2°C.

variation, a concentration of points around the dotted line is apparent. In view of the melting process that might trigger a landslide, maximum radiation values seem to be important as they indicate maximum energy input. The points with maximum solar radiation are more concentrated than the mean and minimum points. Considering the fact that the cold event at Fletschhorn occurred as a combined rock/ice avalanche and that events with positive rock temperature might have been influenced by hydraulic conditions in warm permafrost above the scarp (as in the case of the Randa-event), the concentration becomes clearer.

Parameterized temperatures range from −9.7°C to 3.3°C. As in the first approach, the coldest scarp is the Fletschhorn followed by the Matterhorn. Randa, Val Pola, Druesberg and Zuetribistock show positive temperatures. The other events vary between −6.4°C and 1.8°C. About 84% of the events have a surface temperature between −6° and +2° and 47% between −4° and 2°C. Temperatures calculated with the second approach are lower than those calculated with the first. The difference ranges from 0.3° up to 5.5°C and indicates the importance of complex 3D-topological effects (mountain shadow) reflected in the second approach but not in the first.

Table 3. Potential direct solar radiation and estimated surface temperatures determined by PERMAMAP. ± indicates the range of T2 to the upper/lower boundary of the scarp.

n.	Name	Hlim	T2(°C)	±(°C)
1	Triolet	2523	−5.26	1.2
2	Fletschhorn	2069	−9.67	0.6
3	Brenva I	2769	−6.64	2.0
4	Felik	2883	−3.61	0.6
5	Jungfrau	2821	−5.57	0.3
6	Matterhorn	2353	−9.28	1.5
7	Miage I	1914	−5.62	1.2
8	Becca di Luseney	2817	−1.25	0.8
9	Druesberg	2408	2.03	0.2
10	Val Pola	2474	1.81	1.2
11	Tschierva	2987	−1.42	0.2
12	Piz Scerscen	2918	−4.10	0.6
13	Randa	2601	3.31	1.5
14	Miage II	2120	−4.98	0.3
15a	Zuetribistock I	2191	0.33	0.8
15b	Zuetribistock II	2352	1.39	0.6
16	Brenva II	2894	−4.09	0.9
7	Mättenberg	2370	−1.50	0.6
18	Zugspitze	–	–	–
19	Monte Rosa	2117	−5.60	0.3
20	Gruben	2518	−5.77	0.2

The fact that the temperature calculations are based on statistical relations gained from BTS-measurements remains the main uncertainty of the methods applied. Thermal conditions in rock walls likely are different than those in snow-covered slopes as snow has an insulating effect on rock surface-temperatures. The first systematic study of the spatial distribution of rock temperatures in the Swiss Alps is published by Gruber et al. (2003, this issue). First results indicate that the lower limit of permafrost is higher in rock walls than in more gentle terrain and that aspect-related differences are even more important. Therefore, surface temperatures presented here might be underestimated, especially those of scarps with very steep slope angles and southern expositions.

4.2 *Slope*

As Table 4 shows, the frequency of failure is highest on very steep terrain with mean gradients ranging from 30° to 75°. About 65% of the rock-falls occurred on slopes with mean slope angles of more than 50°.

When looking at critical factors the maximum slope is the determining factor. The maximum slope ranges from 46° to 82°. For 90% of the events the steepest part of the scarp has a maximum gradient of more than 50°, for 80% more than 55° and for 55% more than 60°.

5 DISCUSSION

Many rock-fall events that have occurred during the last hundred years started from rock slopes with permafrost conditions. Therefore, permafrost-related processes have to be considered when evaluating the stability of steep rock walls. Many failures occurred in warm permafrost areas (Scerscen, Tschierva, Mättenberg, Brenva II, Felik or Becca di Luseney – to name a few) and a concentration in these areas is indicated. The starting zones of Randa, Val Pola and (partially) Zuetribistock are located outside permafrost. Ice-blocks were observed on the deposits of the Val Pola-event but not of the other two. In all three cases, however, permafrost occurrence above the scarp might have influenced the water regime and helped trigger the landslide. The processes involved in activating these events might, thus, be related to permafrost in an indirect way.

As permafrost temperatures in the Alps show a clear upward trend (Vonder Mühll et al. 1998), warming permafrost could lead to an increase of permafrost-related slope instabilities. However, events situated in cold permafrost areas have been observed, too. Thus, warm permafrost alone is not a necessary factor for all slope failures in periglacial areas and colder regions, but it cannot be disregarded when investigating slope instabilities.

Table 4. Maximum and mean slope of the starting zones.

n.	Name	Mean (°)	Max (°)
1	Triolet	60.75	64.59
2	Fletschhorn	48.29	55.21
3	Brenva I	65.41	69.88
4	Felik	37.94	47.62
5	Jungfrau	61.41	67.06
6	Matterhorn	75.20	81.90
7	Miage I	44.48	52.78
8	Becca di Luseney	37.82	48.61
9	Druesberg	55.76	69.95
10	Val Pola	30.00	45.60
11	Tschierva	51.80	56.91
12	Piz Scerscen	63.16	71.30
13	Randa	53.59	73.15
14	Miage II	53.03	56.51
15a	Zuetribistock I	73.69	76.90
15b	Zuetribistock II	64.41	76.37
16	Brenva II	47.52	55.73
17	Mättenberg	41.99	60.37
18	Zugspitze	60.00	70.00
19	Monte Rosa	45.09	50.70
20	Gruben	50.50	55.49

Permafrost never acts as the only decisive factor in triggering a landslide. Factors such as steep slopes (all events occurred in steep rock walls), geology (lithology, layer dipping and discontinuities) and the regime, pressure and supply of water play important roles. These factors and combinations of factors have to be investigated in connection with permafrost conditions. Spatial models of critical rock-fall factors then might serve as a basis for assessing hazard potentials that may evolve from periglacial rock falls in case of continued or even accelerated atmospheric temperature rise.

6 CONCLUSIONS AND PERSPECTIVES

Determination of the parameters scarp temperature and slope of known rock-fall events in the Alps provide the following primary results:

- The starting zone of many rock falls that occurred during the last hundred years are located in the permafrost altitudinal belt. Therefore, permafrost-related processes have to be considered when evaluating the stability of steep rock walls. Despite the considerable scatter in the data, a concentration of instabilities in warm permafrost is indicated.
- Some events are situated in cold rock slopes. Therefore, cold permafrost areas cannot be considered to be stable because of low temperature alone.
- Permafrost may influence the water regime of the lower parts of a mountain: Starting zones below the local permafrost limit can thus be influenced by permafrost above the detachment zone.
- In view of the melting process that might trigger a landslide, maximum radiation values seem to be the most important radiation values as they indicate maximum energy input.
- Effects from complex 3D-topological relations (mountain shadow) must be considered in order to estimate realistic temperature conditions within starting zones of rock falls.
- Slope failure occurs mainly on slopes with maximum gradients of more than 50°.

In view of present atmospheric warming and the increasing importance of high mountain resorts as recreation areas, further research is needed. In order to continue the present study surface temperatures will be determined using Gruber et al.'s (2003, this issue) model of spatial distribution of Alpine rock-face temperatures based on measurements in steep rock walls that is currently being developed. This model will likely provide more accurate temperature values for steep scarps than a BTS-based model. Additional factors and combinations of factors as well as altitude difference, length, overall slope and surface characteristics (glacier, moraines, obstacles, etc.) of runout

paths will also be inventoried. Because of the low friction offered by ice to sliding, runout paths are around 24% longer in glacial than in non-glacial environments (Deline 2001). Evans & Clague's (1988) formula for glacial and non-glacial environments will be applied and additional models will be tested.

REFERENCES

Alean, J. 1984. Ice avalanches and a landslide on Grosser Aletschgletscher. *Zeitschrift für Gletscherkunde und Glazialgeologie* 20: 9–25.

Coaz, J.F. 1910. *Statistik und Verbau der Lawinen in den Schweizeralpen*. Bern: Stämpfli.

Davies, M., Hamza, O. & Harris, C. 2001. The effect of rise in mean annual air temperature on the stability of rock slopes containing ice-filles discontinuities. *Permafrost and Periglacial Processes* 12: 137–144.

Deline, P. 2001. Recent Brenva rock avalanches (Valley of Aosta): New chapter in an old story? *Suppl. Geogr. Fis. Dinam. Quat.* V (2001): 55–63.

Deline, P. 2002. Etude géomorphologique des interactions écroulment rocheux/glaciers dans la haute montagne alpine (versant sud-est du massif Mont Blanc). Savoie: Dissertation, Universitié de Savoie.

Dramis, F., Govi, M., Guglielmin, M. & Mortara, G. 1995. Mountain permafrost and slope instability in the Italian Alps: the Val Pola landslide. *Permafrost and Periglacial Processes* 6: 73–82.

Dutto, F. & Mortara, G. 1991. Grandi frane storiche con percorso su ghiacciaio in Valle d'Aosta. *Rev. Valdôtaine Hist. Nat*. 45: 21–35.

Evans, S.G. & Clague, J.J. 1988. Catastrophic rock avalanches in glacial environment. *Landslides. Lausanne: Proceedings of the fifth International Symposium on Landslides, 10–15 July 1988* 2: 1153–1158.

Frauenfelder, R. & Kääb, A. 2000. Towards a paleoclimatic model of rock-glacier formation in the Swiss Alps. *Annals of Glaciology* 31: 281–286.

Frauenfelder, R., Haeberli, W., Hoelzle, M. & Maisch, M. 2001. Using relict rockglaciers in GIS-based modelling to reconstruct Younger Dryas permafrost distribution patterns in the Err-Julier area, Swiss Alps. *Norsk Geografisk Tidsskrift* 55: 195–202.

Funk, M. & Hoelzle, M. 1992. Application of potential direct solar radiation model for investigating occurrences of mountain permafrost. *Permafrost and Periglacial Processes* 3(2): 139–142.

Geotest 2000, unpubl. *Grindelwald, Mättenberg-Ankenbälli, Felssturz vom 8. 9. 2000*. Zollikofen: Bericht Nr. 00195.1.

Gruber, S., Peter, M., Hoelzle, M., Woodhatch, I. & Haeberli, W. 2003, in press. Surface temperatures in steep Alpine rock faces – a strategy for regional-scale measurements and modelling. *This issue*.

Haeberli, W. 1975. *Untersuchungen zur Verbreitung von Permafrost zwischen Flüelapass und Piz Grialetsch (Graubünden)*. Zürich: Mitteilung Nr. 17 der Versuchsanstalt für Wasserbau, Hydrologie und Glaziologie der ETH Zürich.

Haeberli, W., Wegmann, M. & Vonder Mühll, D. 1997. Slope stability problems related to glacier shrinkage and permafrost degradation in the Alps. *Eclogae geologicae Helveticae* 90: 407–414.

Hoelzle, M. & Haeberli, W. 1995. Simulating the effects of mean annual air temperature changes on permafrost distribution and glacier size. An example from the Upper Engadin, Swiss Alps. *Annals of Glaciology* 21: 400–405.

Hoelzle, M. 1996. Mapping and modelling of mountain permafrost distribution in the Alps. *Norsk Geografisk Tidsskrift* 50: 11–15.

Keller, F. 1992. Automated mapping of permafrost using the program PERMAKART within the geographical information system ARC/INFO. *Permafrost and Periglacial Processes* 3(2): 133–138.

Keller, F. 1996, unpubl. *Glaziologische Aspekte zum Berg sturz Sandalp-Zuetribistock (GL) 1996*. Samedan: Untersuchungs bericht des Baustab Geb AK 3.

Kobel, M. 1996, unpubl. *Bergsturz Sandalp: geologische Begutachtung*. Bericht Nr. 4428–1, 20 Februar 1996. Sargans: Dr. M. Kobel und Partner AG.

Mittaz, C., Hoelzle, M. & Haeberli, W. 2000. First results and interpretation of energy-flux measurements of Alpine permafrost. *Annals of Glaciology* 31: 275–280.

Mittaz, C., Imhof, M., Hoelzle, M. & Haeberli, W. 2002. Snowmelt evolution mapping using an energy balance approach over an alpine terrain. *Arctic, Antarctic and Alpine Research* 34(2): 274–281.

Noetzli, J. 2003, unpubl. GIS-basierte Modellierung von Felsstürzen über Gletschern. Zürich: Diplomarbeit, Geographisches Institut, Universität Zürich.

Porter, S.C. & Orombelli, G. 1980. Catastrophic rockfall of September 12, 1717 on the Italian flank of the Mont Blanc massif. *Zeitschrift für Geomorphologie* 24: 200–218.

Schindler, C., Cuénod, Y., Eisenlohr, T. & Joris, C.-J. 1993. Die Ereignisse vom 18. April und 9. Mai 1991 bei Randa (VS) – ein atypischer Bergsturz in Raten. *Eclogae geologicae Helveticae* 86: 643–665.

Schweizer, J. 1990, unpubl. *Short note on the rockslide to Tschiervagletscher*, 29. October 1988. Davos.

Vanni, M. 1943. La frana del Cervino del 9 Iuglio e del 18 agosto 1943. *Boll. Soc. Geogr. It., ser. VII* 8(6): 362–363.

Vonder Mühll, D., Stucki, T. & Haeberli, W. 1998. Borehole temperatures in Alpine permafrost: a ten year series. In: *Proceedings of the Seventh International Conference on Permafrost. Yellowknife, Canada:* Nordicana 57: 1089–1095.

Wegmann, G. 1995, unpubl. *Permafrostvorkommen auf geringer Meereshöhe – eine Fallstudie im Brüeltobel (AI)*. Zürich: Diplomarbeit Geographisches Institut, Universität Zürich.

Wegmann, M. 1998. *Frostdynamik in hochalpinen Felswänden am Beispiel der Region Jungfraujoch – Aletsch*. Zürich: Mitteilung Nr. 161 der Versuchsanstalt für Wasserbau, Hydrologie und Glaziologie der ETH Zürich.